Supporting Information

In Situ Topochemically Converted 2-D $BaTiO_3$ Polycrystals with Multifarious Zone Axes

Fang Kang[†, ‡, ※], Bin Yao[⍰, ※], Wenxiong Zhang[§], Fangyi Yao[ϕ], Qing Zhao[†], Lei Miao[†], Fan Zhao[†, ¬], Zhuonan Huang[*, †], Weixing Zhao[†, ϕ], Galhenage Asha Sewvandi[Π], Yifei Wang[*, ‡], Lixue Zhang[‡], Qi Feng[ϕ], Dengwei Hu[*, †]

[†] Faculty of Chemistry and Chemical Engineering, Engineering Research Center of Advanced Ferroelectric Functional Materials, Key Laboratory of Phytochemistry of Shaanxi Province, Baoji University of Arts and Sciences, 1 Hi-Tech Avenue, Baoji, Shaanxi, 721013, China

[‡] State Key Laboratory for Mechanical Behavior of Materials, School of Materials Science and Engineering, Xi'an Jiaotong University, Xi'an, 710049, China

[⍰] School of Aerospace Science & Technology, Xidian University, Xi'an, 710071, P.R. China

[¬] School of Microelectronics, Xi'an Jiaotong University, Xi'an 710049, China.

[§] Institute for Solid State Physics, The University of Tokyo, Koto, Sayo, Hyogo 679-5148, Japan

[ϕ] Department of Advanced Materials Science, Faculty of Engineering and Design, Kagawa University, 2217-20 Hayashi-cho, Takamatsu-shi, 761-0396 Japan

[Π] Department of Materials Science and Engineering, Faculty of Engineering, University of Moratuwa, Katubedda, Sri Lanka

[⁑] Electrical Insulation Research Center, Institute of Materials Science, University of Connecticut, 97 N Eagleville Rd, Storrs, CT 06269, USA

[※] These authors contributed equally to this work.

KEYWORDS: Polycrystals; In situ topochemical conversion; Piezoelectric properties; Textured materials

Multi-crystal-oriented $BaTiO_3$ polycrystals with a dominant [100] direction can be *in situ* topochemically converted from HTO crystals *via* calcination process.

Corresponding Authors

E-mail: iceedu@126.com (Z. Huang); y.wang@uconn.edu (Y. Wang); hdwpolymer@yahoo.co.jp (D. Hu); Fax: +86 (0)917-356-6366; Tel: +86 (0)917-356-6055

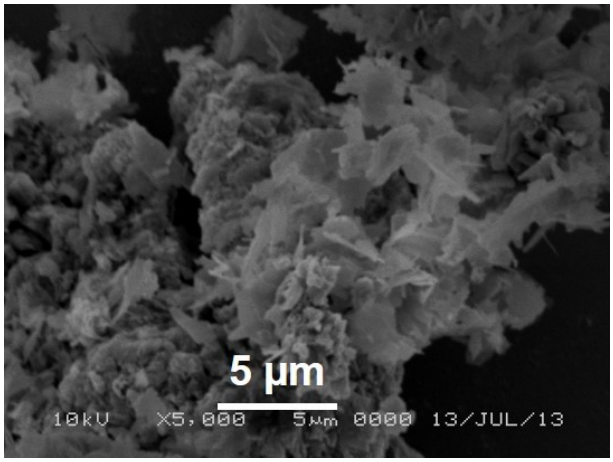

Figure S1 SEM image of specimen obtained by the calcination of HTO and $Ba(OH)_2 \cdot 8H_2O$ mixture powders at 600°C for 3 h.

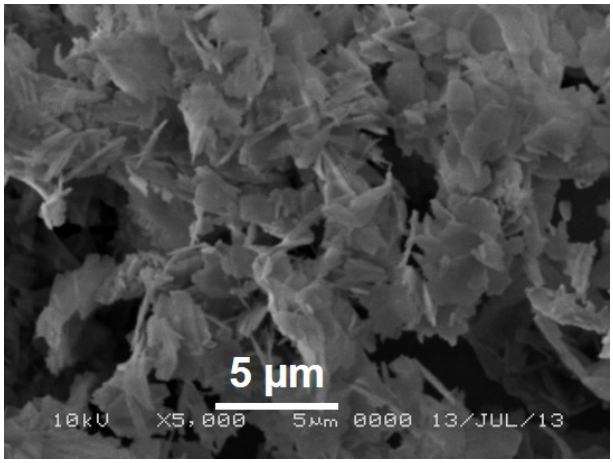

Figure S2 SEM images of specimens obtained by the calcination of HTO and $Ba(Ac)_2$ mixed powders at 600 °C for 3 h.

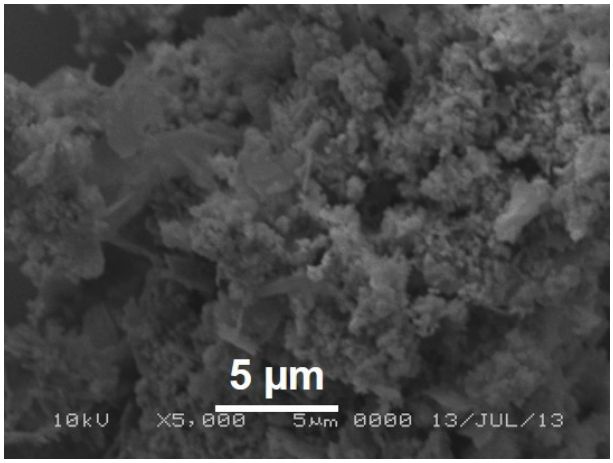

Figure S3 SEM images of specimens obtained by the calcination of HTO and $Ba(NO_3)_2$ mixed powders at 600 °C for 3 h.

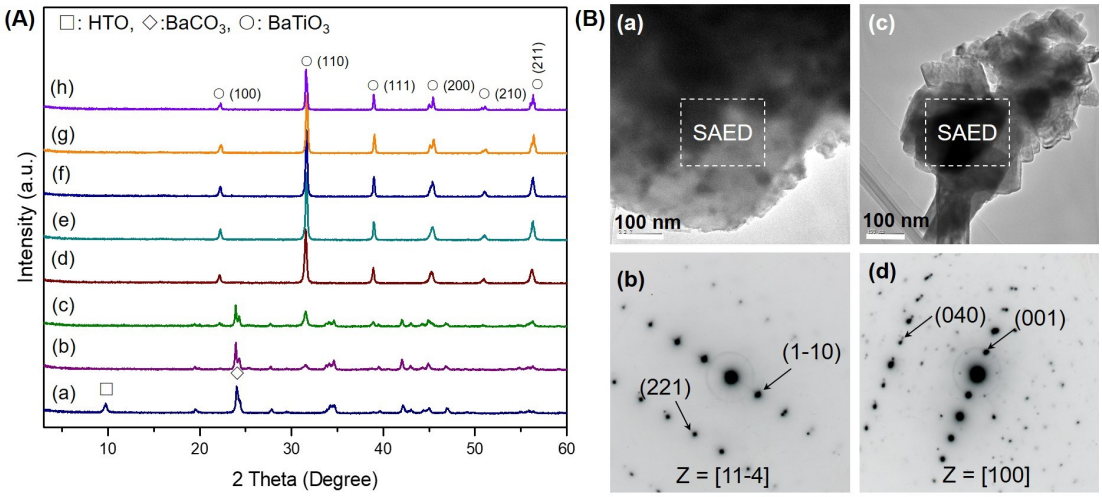

Figure S4 (A) XRD patterns of specimens of HTO-$BaCO_3$ mixtures (a) before and (b-h) after calcinations at (b) 600, (c) 700, (d) 800, (e) 900, (f) 1000, (g) 1150, and (h) 1200 °C for 3 h. **(B)** (a, c) TEM images and (b, d) SAED patters of specimens obtained by the calcination of HTO-$BaCO_3$ mixed powders at 800 °C for 3h.

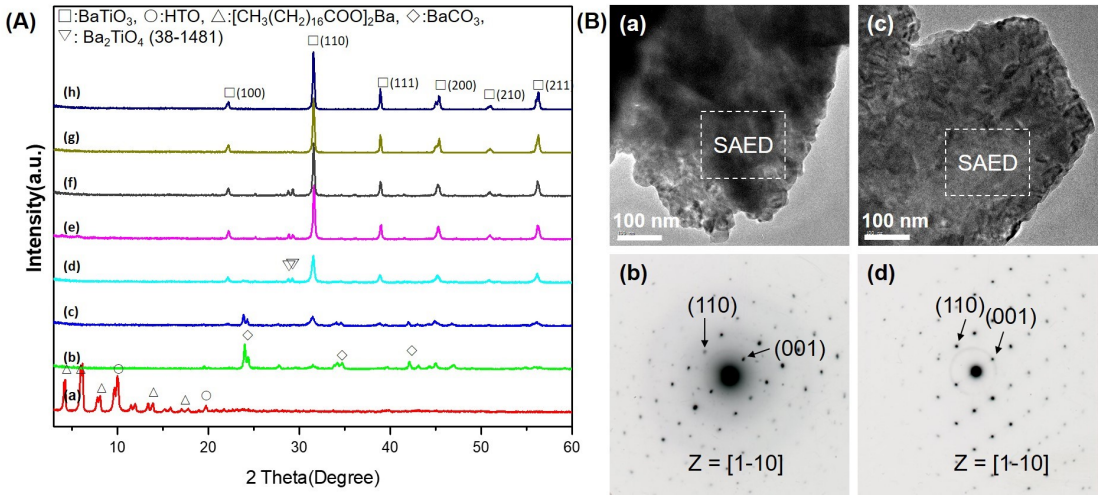

Figure S5. (A) XRD patterns of specimens of the HTO-$Ba[CH_3(CH_2)_{16}COO]_2$ mixtures (a) before and after calcinations at (b) 600, (c) 700, (d) 800, (e) 900, (f) 1000, (g) 1100, and (h) 1200 oC for 3 h, respectively. (B) (a, c) TEM images and (b, d) SAED patterns of specimens obtained by calcination of HTO-$Ba[CH_3(CH_2)_{16}COO]_2$ mixed powders at 800 °C for 3h.

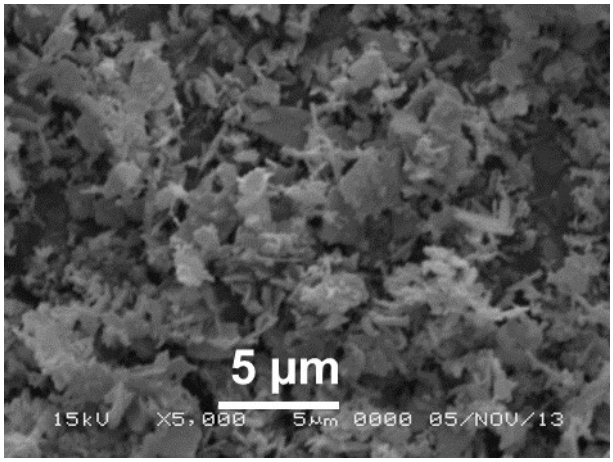

Figure S6. SEM images of specimens of HTO-$BaCO_3$ mixtures after calcinations at 800 °C for 3h.

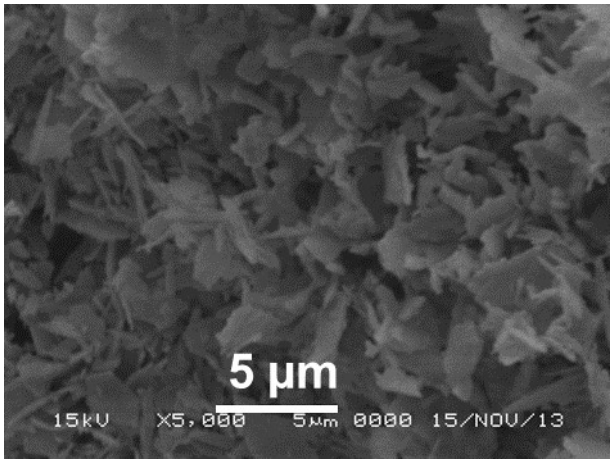

Figure S7. SEM images of specimens of HTO-$Ba[CH_3(CH_2)_{16}COO]_2$ mixtures after calcinations at 900 °C for 3h.

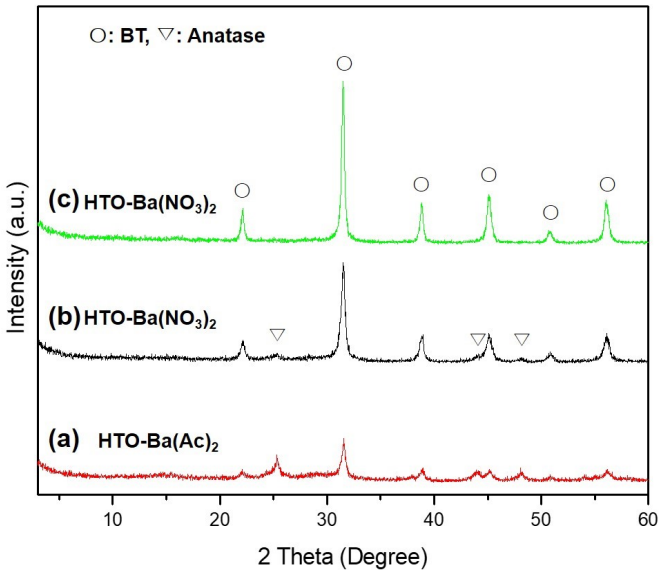

Figure S8. XRD patterns of specimens obtained by the calcination of HTO and (a) $Ba(Ac)_2$ and (b,

c) $Ba(NO_3)_2$ mixed powders at 500 °C for (a, b) 15 h and (c) 18 h.

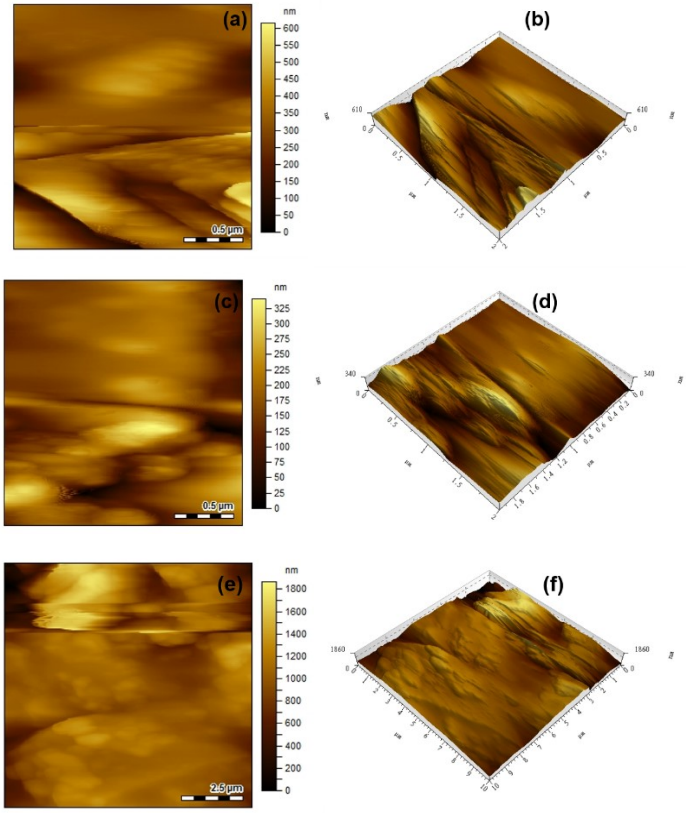

Figure S9 (a, c, e) 2D and (b, d, f) 3D AFM images with the range of 0.5 μm × 0.5 μm of specimens obtained by the calcination of (a, b) HTO and $Ba(Ac)_2$ mixture, (c, d) HTO and $Ba(NO_3)_2$ at 500°C for 15 h, and (e) 2D and (f) 3D images with the range of 0.5 μm × 0.5 μm of specimens obtained by the calcination of HTO and $Ba(NO_3)_2$ at 500 °C for 18 h.

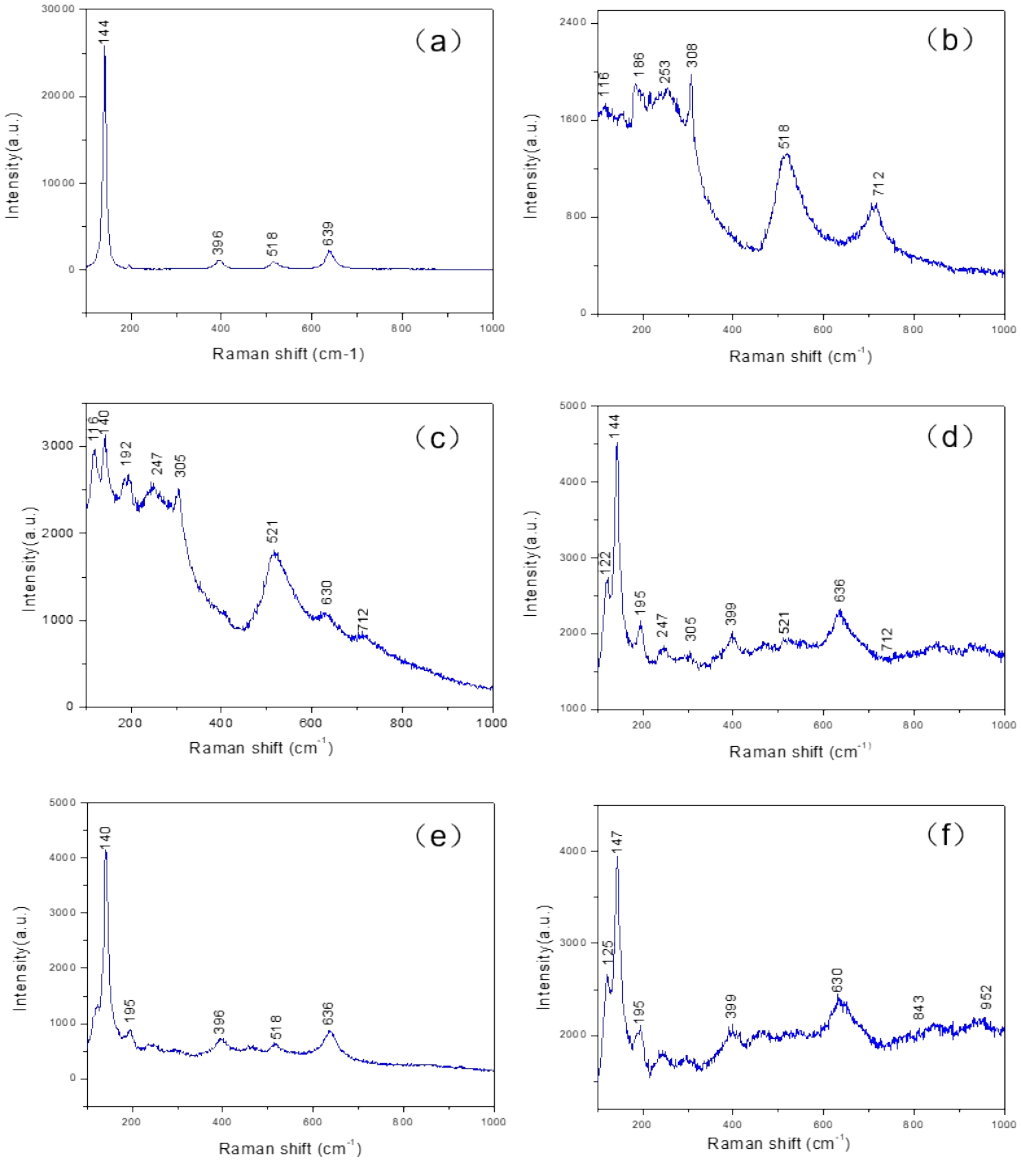

Figure S10 Raman spectra of (a) anatase TiO_2 and specimens obtained from the reaction systems of (b) HTO-$Ba(NO_3)_2$, (c) HTO-$Ba(OH)_2$, (d) HTO-$Ba(Ac)_2$, (e) HTO-$BaCO_3$, and (f) HTO-$Ba[CH_3(CH_2)_{16}COO]_2$ at 600 °C for 3 h.

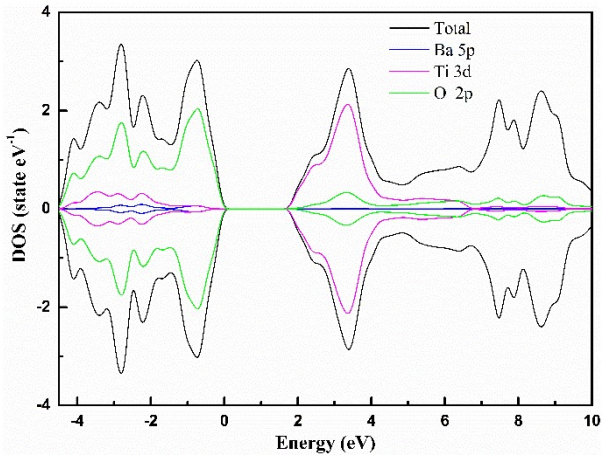

Figure S11. Total and partial densities of states for tetragonal $BaTiO_3$. The Fermi level is set to zero. The optimized lattice parameters for the $BaTiO_3$ are a = b = 4.052 Å, c = 4.066 Å. These values are very close to the experimental data: a = 3.9998 Å and c = 4.0180 Å[i]. As seen from Figure 7, the calculated band gap (within GGA+U) of $BaTiO_3$ is about 2.12 eV which is smaller than that of experimental result (3.2 eV). The underestimation of band gap can be predicted due to the known defects of the DFT methodology. However, there is 13.9% improvement for band gap compared with the standard DFT result of 1.86 eV as the intra-site Coulomb repulsion U-term is added. The valence-band maximum (VBM) mainly consists of O 2p states and a small contribution of the Ti 3d and Ba 5p states, whereas the conduction-band minimum (CBM) is composed of a mixture of Ti 3d and O 2p states, indicating the strong hybridization between the Ti 3d and O 2p states for the tetragonal $BaTiO_3$.

Table S1 Zone axes of platelike BT mesocrystals obtained by the calcination of HTO and $Ba(OH)_2$ mixture at 600 °C for 3 h.

Serial number	1	2	3	4	5	6	7
Zone axis/Crystal-axis orientations	[13-5]	**[110]**	**[100]**	[121]	[115]	[111]	Unknown[a]
Number of occurrences	1	4	13	1	1	2	2
Occurrence probability	4.2%	16.7%	54.2%	4.2%	4.2%	8.3%	8.3%

[a]The diffraction spots are too chaotic to determine the zone axis. The following is the same.

Table S2 Zone axes of platelike BT mesocrystals obtained by the calcination of HTO and $Ba(Ac)_2$ mixture at 600 °C for 3 h.

Serial number	1	2	3	4	5	6
Zone axis/Crystal-axis orientations	[-111]	**[110]**	[12-4]	[112]	**[100]**	Unknown
Number of occurrences	2	3	1	1	6	1
Occurrence probability	14.3%	21.4%	7.1%	7.1%	42.9%	7.1%

Table S3 Zone axes of platelike BT mesocrystals obtained by the calcination of HTO and $Ba(NO_3)_2$ mixture at 600 °C for 3 h.

Serial number	1	2	3	4	5	6	7
Zone axis/Crystal-axis orientations	[114]	**[100]**	[11-3]	[-215]	**[110]**	[-213]	Unknown
Number of occurrences	1	15	2	1	4	1	1
Occurrence probability	4%	60%	8%	4%	16%	4%	4%

Table S4 Zone axes of platelike BT mesocrystals obtained by the calcination of HTO and $Ba[CH_3(CH_2)_{16}COO]_2$ mixture at 800 °C for 3 h.

Serial number	1	2	3	4	5	6
Zone axis/Crystal-axis orientations	[-112]	**[110]**	[-114]	[-113]	**[100]**	[123]
Number of occurrences	1	4	4	1	6	1
Occurrence probability	5.9%	23.5%	23.5%	5.9%	35.3%	5.9%

Table S5 Zone axes of platelike BT mesocrystals obtained by the calcination of HTO and $Ba(NO_3)_2$ mixture at 500 °C for 18 h.

Serial number	1	2	3	4
Zone axis/Crystal-axis orientations	**[100]**	**[110]**	[-215]	[-112]
Number of occurrences	10	3	1	1
Occurrence probability	67%	20%	7%	7%